PHYSICAL REVIEW E **91**, 061001(R) (2015)

# Predicting the Knudsen paradox in long capillaries by decomposing the flow into ballistic and collision parts

Giorgos Tatsios,[1] Stefan K. Stefanov,[2] and Dimitris Valougeorgis[1]
[1]*Department of Mechanical Engineering, University of Thessaly, Volos, Greece*
[2]*Institute of Mechanics, Bulgarian Academy of Sciences, Sofia, Bulgaria*
(Received 18 March 2015; published 10 June 2015)

The well-known Knudsen paradox observed in pressure driven rarefied gas flows through long capillaries is quantitatively explored by decomposing the particle distribution function into its ballistic and collision parts. The classical channel, tube, and duct Poiseuille flows are considered. The solution is obtained by a typical direct simulation Monte Carlo algorithm supplemented by a suitable particle decomposition indexation process. It is computationally confirmed that in the free-molecular and early transition regimes the reduction rate of the ballistic flow is larger than the increase rate of the collision flow deducing the Knudsen minimum of the overall flow. This description interprets in a precise, quantitative manner the appearance of the Knudsen minimum and verifies previously reported qualitative physical arguments.

DOI: 10.1103/PhysRevE.91.061001 PACS number(s): 47.45.−n, 05.20.Dd, 51.10.+y, 47.45.Ab

Internal rarefied gas flow in a wide range of the Knudsen number was first studied experimentally and theoretically by Knudsen, who examined the dependence of the conductance at different pressure and geometrical parameters [1]. Considering a tube much longer than its radius, he developed an expression for the tube conductance and observed a conductance minimum at Kn $\simeq 1$, well known as the *Knudsen minimum* or the *Knudsen paradox*.

Over the years Knudsen's results have been improved, extended, and generalized. The steady isothermal gas flow through long capillaries still remains an active research topic and a subject of many investigations [2–17]. Recently, simple closed-form expressions for the reduced flow rate in long tubes in all flow regimes were deduced in [18] and [19] based on direct simulation Monte Carlo (DSMC) and kinetic simulations, respectively. These formulas, as the one in [1], produce the Knudsen minimum, indicating that the conductance (or the reduced flow rate) lies below the corresponding free-molecular values over a range of pressures in the transition regime.

A qualitative explanation for the conductance minimum in a long capillary has been suggested by Polland and Present [20]. They considered two groups of molecules flowing across a differential cross section of the capillary. The first one consists of particles which arrived from the boundaries with no collisions and the second one of particles which experienced at least one collision. At zero pressure the total flow comes from particles only of the first group, while as the pressure is increased to small values the flow of the first group particles is decreased because of the obstruction of the long particle paths by the added molecules. In parallel the flow of the second group particles is increased through the development of a drift transport due to intermolecular collisions. The authors claim that at small pressures the rate of reduction of the first flow is larger than the rate of increase of the second one and therefore the total flow must initially decrease with pressure. A further increase in pressure stimulates the overall drift velocity that in turn, from that point on, monotonically increases the entire flow through the tube.

Recently, the concept of decomposing the solution into two parts, as described above, has been accordingly implemented in the typical DSMC algorithm by introducing a suitable particle indexation process [21,22]. In the present work the same DSMC decomposition is implemented to investigate the Knudsen paradox in a precise manner with quantitative arguments.

Consider the classical pressure driven isothermal flow of a rarefied gas at a reference temperature $T_0$ through a capillary of length $L$ with the pressure at the inlet and outlet of the capillary maintained at $P_1$ and $P_2$, respectively ($P_1 > P_2$). The area and the perimeter of the capillary cross section are denoted by $A'$ and $\Gamma'$, respectively. The $z'$ axis is taken along the capillary and the cross section is on the $(x',y')$ plane. The characteristic length of the cross section, denoted by $H$, is assumed to be much smaller than its length ($H/L \ll 1$). In this case, as rigorously proved in [23], the pressure (and density) is constant on each cross section and varies only along the capillary in the flow direction, i.e., $P = P(z') \in [P_1, P_2]$ and the flow is considered as fully developed in the $z'$ direction.

The basic flow parameter is the Knudsen number (Kn) or alternatively the rarefaction parameter ($\delta$), defined as

$$\delta = \frac{H P_0}{\mu_0 \upsilon_0} \sim \frac{1}{\mathrm{Kn}} = \frac{\lambda}{H}, \tag{1}$$

where $P_0 = (P_1 + P_2)/2$ is the reference pressure, $H$ is the characteristic length, $\mu_0$ is the gas viscosity at $T_0$, $\upsilon_0 = \sqrt{2k_B T_0/m}$ is the most probable molecular velocity ($k_B$ is the Boltzmann constant and $m$ the molecular mass), and $\lambda$ denotes the mean free path. It is convenient to introduce the dimensionless variables $x = x'/H$, $y = y'/H$, $z = z'/H$, the dimensionless cross section $A = A'/H^2$ and perimeter $\Gamma = \Gamma'/H$, as well as the dimensionless bulk velocity in the $z'$ direction $u(x,y) = u'(x',y')/(\upsilon_0 X_P)$ (the other two velocity components are zero) and shear stresses $\tau_{\alpha z}(x,y) = \tau'_{\alpha z}(x',y')/(2X_P P_0), \alpha = x,y$, where $X_P = (dP/dz)/P_0$ is the local pressure gradient.

A quantity of major importance is the kinetic coefficient (or reduced flow rate) $G$, which is defined according to

$$G = \frac{2}{A}\int_A u(x,y)dA. \tag{2}$$

 ©2015 American Physical Society

The variation of $G$ in terms of $\delta$ for gas flows through long capillaries of various cross sections has been a focal point of investigation and tabulated results are available in the literature [2,3,5,6,8,24–27]. The Knudsen minimum always appears in the transition regime and the exact value of $\delta$ where the minimum occurs depends on the capillary cross section and the gas-surface accommodation coefficient.

The average shear stress at the wall is also introduced to be later used for benchmarking purposes. Since the flow is fully developed and there is no net momentum flux in the flow direction, the net pressure and the wall shear stress are equated to yield $\bar{\tau}'_w = (A'/\Gamma')(dP/dz')$. This expression is nondimensionalized and it is deduced that $\bar{\tau}_w = \bar{\tau}'_w/(2P_0X_P) = A/(2\Gamma) = 0.25$ [7,27]. This result is always valid independent of the channel cross section and the rarefaction parameter $\delta$ and therefore it may be used as a benchmark to test the accuracy of the DSMC calculations.

The flow is simulated based on the Boltzmann equation which is solved via the DSMC method subject to the no time counter (NTC) scheme proposed by Bird [28]. The flow is simulated only on the capillary cross section pushed by a uniform force in the flow direction resulting in a dimensionless acceleration equal to $X_P/2$ acting on each gas molecule. It is noted that $X_P$ is a constant taking sufficiently small values to ensure the linearity of the flow. The main unknown is averaged over a time interval dimensionless distribution function in a cell, denoted by $g(x,y,\zeta)$, where $(x,y)$ are the cell space coordinates and $\zeta = [\zeta_x,\zeta_y,\zeta_z]$ is the molecular velocity vector. This function is expressed as

$$g(x,y,\zeta) = \frac{1}{SV_{Cell}} \sum_{k=1}^{S} \sum_{i=1}^{N(t_k)} \delta(\zeta - \zeta_i(t_k)), \tag{3}$$

where $V_{Cell}$ is the volume of each cell, $\delta(\zeta - \zeta_i(t_k))$ denotes the Dirac delta function, $S$ denotes the number of samples, $t_k$ indicates the different times over which the sampling is performed, and $N(t_k)$ is the number of particles in the cell at time $t_k$. The total number of sampled particles is $N_T = \sum_{k=1}^{S} N(t_k)$.

Furthermore, the decomposition introduced in [19] is applied and the distribution function is decomposed as

$$g\,(x,y,\zeta) = g^{(b)}\,(x,y,\zeta) + g^{(c)}\,(x,y,\zeta)\,, \tag{4}$$

where

$$g^{(b)}(x,y,\zeta) = \frac{1}{SV_{Cell}} \sum_{k=1}^{S} \sum_{i=1}^{N(t_k)} [1 - I_i(t_k)]\,\delta\,(\zeta - \zeta_i\,(t_k)), \tag{5}$$

and

$$g^{(c)}(x,y,\zeta) = \frac{1}{SV_{Cell}} \sum_{k=1}^{S} \sum_{i=1}^{N(t_k)} I_i(t_k)\delta\,(\zeta - \zeta_i\,(t_k)) \tag{6}$$

denote the ballistic and collision parts of the distribution function, respectively, with $I_i(t_k)$ being an indicator which has the value of 0 or 1 indicating if a particle contributes to the ballistic or the collision distribution, respectively.

As described in [19], each time that a particle is reflected from the wall its indicator is set to 0. In the stage of free motion the indicators are not changed. In the stage of binary collisions the indicators $(I_l, I_m)$ of any pair of particles $(l,m)$ involved in a collision are set to 1. During the simulation process the particle indicators may change their values all the time. In the sampling stage of the macroscopic properties at some given time, particles with indicators $I_i = 0$ and $I_i = 1$, $i = 1,\ldots,N(t_k)$, are considered belonging to the ballistic and collision parts of the particle distribution, respectively. The total number of all particles accumulated in a cell is divided into the ballistic and collision groups as $N_T = N_T^{(b)} + N_T^{(c)}$.

The macroscopic quantities are decomposed into the ballistic and collision parts as $n = n^{(b)} + n^{(c)}$, $u = u^{(b)} + u^{(c)}$ and $\tau_{\alpha z} = \tau_{\alpha z}^{(b)} + \tau_{\alpha z}^{(c)}$, $\alpha = x,y$. By taking the corresponding moments of (5) and (6) and integrating over the velocity space it is deduced that

$$n^{(b)}(x,y) = \frac{N_T^{(b)}}{SV_{Cell}}, \quad n^{(c)}(x,y) = \frac{N_T^{(c)}}{SV_{Cell}}, \tag{7}$$

$$u^{(b)} = \frac{1}{X_P N_T} \sum_{k=1}^{S} \sum_{i=1}^{N(t_k)} [1 - I_i(t_k)]\zeta_{z,i}(t_k),$$

$$u^{(c)} = \frac{1}{X_P N_T} \sum_{k=1}^{S} \sum_{i=1}^{N(t_k)} I_i(t_k)\zeta_{z,i}(t_k), \tag{8}$$

$$\tau_{\alpha z}^{(b)} = \frac{1}{X_P N_T} \sum_{k=1}^{S} \sum_{i=1}^{N(t_k)} [1 - I_i(t_k)]\zeta_{\alpha,i}(t_k)\zeta_{z,i}(t_k) - u_a^{(b)} u_z, \tag{9}$$

$$\tau_{\alpha z}^{(c)} = \frac{1}{X_P N_T} \sum_{k=1}^{S} \sum_{i=1}^{N(t_k)} I_i(t_k)\zeta_{\alpha,i}(t_k)\zeta_{z,i}(t_k) - u_a^{(c)} u_z. \tag{10}$$

Similarly the reduced flow rate is decomposed as $G = G^{(b)} + G^{(c)}$ where $G^{(b)}$ and $G^{(c)}$ are the reduced ballistic and collision flow rates, respectively.

Applying this methodology, four rarefied gas flows through long capillaries, namely the flow between parallel plates (channel flow), through orthogonal ducts with two aspect ratios $H/W = 0.1$ and 1 (duct flow), and through long circular tubes (tube flow) are explored. Purely diffuse boundary conditions are considered and the hard sphere model was used. The physical space domain is discretized using 100 cells per unit length with about 1000 simulator particles per cell. The time step is chosen close to 1/3 of the cell transversal time, defined as $\Delta x'/v_0$. The macroscopic quantities are obtained by time averaging over more than $S = 10^7$ time steps after the steady state has been recovered. By setting the acceleration parameter $X_P/2 = 0.01$ the deduced DSMC solution has the well-known linear characteristics (i.e., the solution is directly proportional to the source term) and nonlinear phenomena are absent. The results presented here are accurate up to at least two significant figures which is adequate for the objectives of the present work.

The flow rates $G^{(b)}$, $G^{(c)}$, and $G$ are plotted in terms of $\delta$ in Fig. 1 for the channel, the duct ($H/W = 0.1$ and 1), and the tube flows. The well-known behavior of $G$ with a minimum in the transition regime is observed [2,6,24,25]. The values of $\delta$ where the Knudsen minimum occurs, denoted by $\delta_{\min}$, are indicated in Fig. 1 and in tabulated form in Table I.

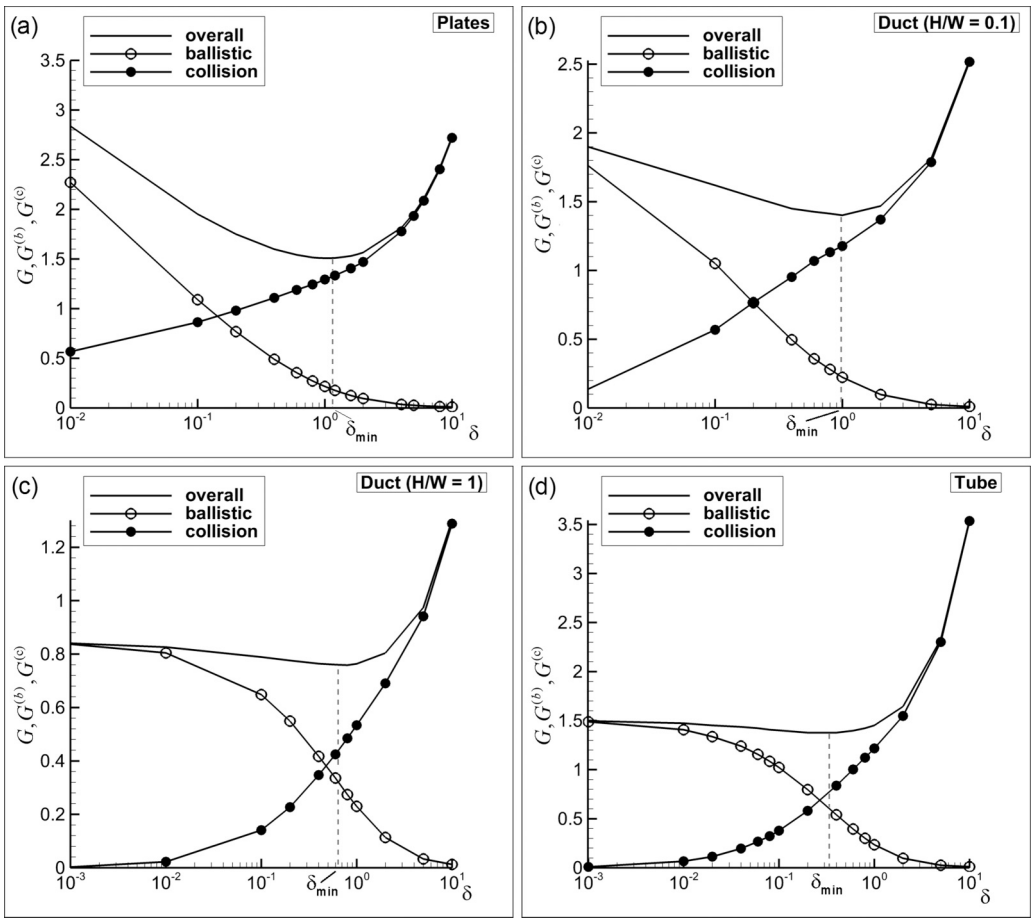


FIG. 1. Ballistic, collision, and overall reduced flow rates in terms of the rarefaction parameter for (a) channel flow, (b) duct flow ($H/W = 0.1$), (c) duct flow ($H/W = 1$), and (d) tube flow.

For the channel flow, a detailed comparison between the results in Fig. 1(a) with the corresponding ones in Table V of [2] has been performed. To achieve that $\delta$ has been related to the parameter $k$ of [2] according to $\delta = 1/(\alpha k)$ with $\alpha = 5/4$ and also the present flow rates have been divided by 2. For all values of $\delta \in [0.1, 10]$ the agreement is excellent with the relative error being less than 0.5%. Based on this comparison and on the previously described formulation it is quantitatively verified that the present "linear" DSMC solution corresponds to the one obtained by solving the same flow configurations based on the linear Boltzmann equation for hard sphere molecules.

In Fig. 1, the ballistic and collision flow rates always have a monotonous behavior with respect to $\delta$. As $\delta$ is increased $G^{(b)}$ constantly decreases and finally diminishes as $\delta \to \infty$, while $G^{(c)}$ initially at $\delta = 0$ is zero and then constantly increases. Thus, at $\delta = 0$ and $\delta \to \infty$ the overall flow rate is $G = G^{(b)}$ and $G = G^{(c)}$ respectively. In the free-molecular and early transition regimes the reduction rate of $G^{(b)}$ is larger than the increase rate of $G^{(c)}$ resulting to the Knudsen minimum of the overall flow $G$.

TABLE I. Values of $\delta_{min}$ for flows through long capillaries of various cross sections.

| Capillary | Channel ($H/W \to 0$) | Duct ($H/W = 0.1$) | Duct ($H/W = 1$) | Tube |
|---|---|---|---|---|
| $\delta_{min}$ | 1.1 | 0.93 | 0.61 | 0.31 |

To further elaborate on this issue, in Fig. 2, the derivatives $dG^{(b)}/d\delta$, $dG^{(c)}/d\delta$, and $dG/d\delta$ are plotted in terms of $\delta$. They are computed numerically based on the results of $G^{(b)}$ and $G^{(c)}$. It is seen that $dG^{(b)}/d\delta$ is always negative and as $\delta$ is increased it tends to zero since $G^{(b)}$ itself is zero. Actually, for $\delta > 5$ there is no contribution of $G^{(b)}$ to $G$. In parallel $dG^{(c)}/d\delta$ is always positive and as $\delta \to \infty$, the $\lim_{\delta\to\infty}(dG^{(c)}/d\delta) = \lim_{\delta\to\infty}(dG/d\delta) = c$. In the hydrodynamic limit, solving the Stokes equation, it is readily deduced that $c = 1/6$ in the channel flow and $c = 0.25$ in the tube flow [24]. The corresponding values in Fig. 2 at $\delta = 10$ are very close to these ones. Furthermore, it is computationally confirmed that

$$\left|\frac{dG^{(b)}}{d\delta}\right| \gtrless \frac{dG^{(c)}}{d\delta} \quad \text{for} \quad \delta \lesseqgtr \delta_{min}. \tag{11}$$

Clearly, this behavior of the derivatives of the two parts leads to a single root of the derivative of the overall reduced flow rate, which is crossing the $\delta$ axis from negative to positive values, indicating the existence of a minimum. Obviously, the value of $\delta = \delta_{min}$ where $dG/d\delta = 0$ is where the Knudsen minimum occurs. This description quantitatively explains

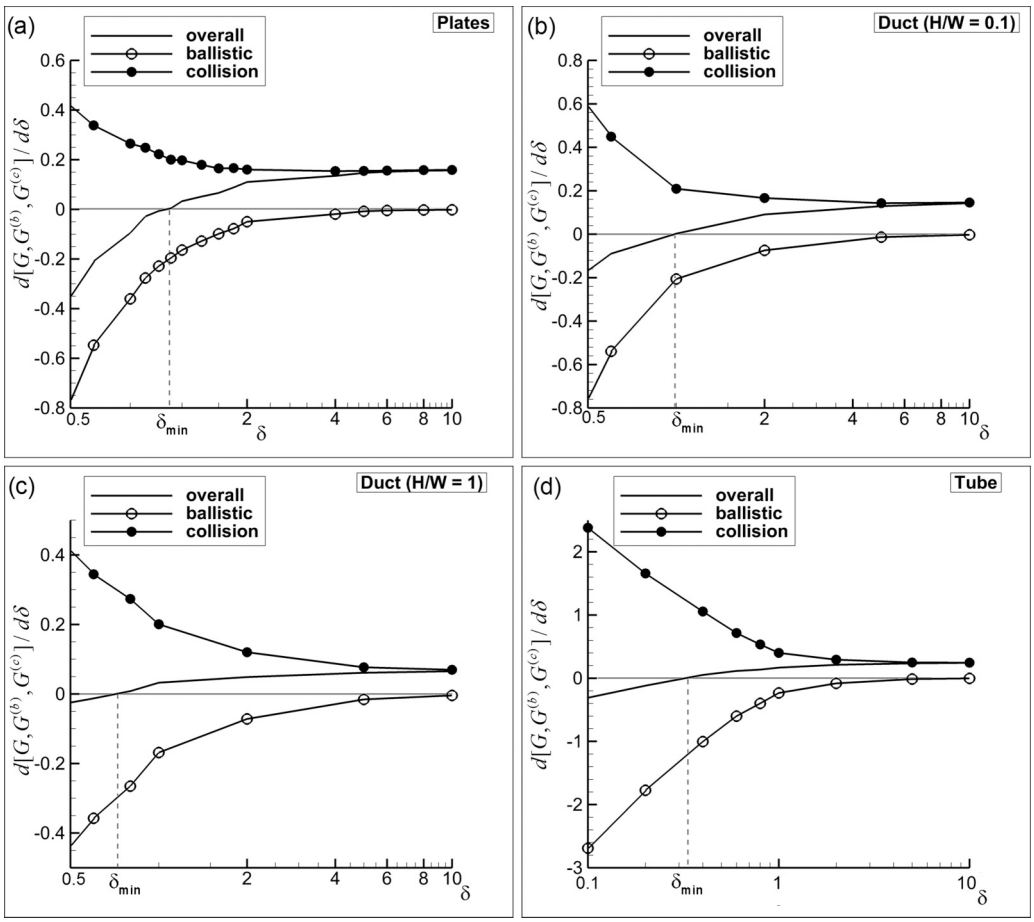


FIG. 2. Derivatives with respect to $\delta$ of the ballistic, collision, and overall reduced flow rates in terms of the rarefaction parameter for (a) channel flow, (b) duct flow ($H/W = 0.1$), (c) duct flow ($H/W = 1$), and (d) tube flow.

the appearance of the Knudsen minimum and verifies the qualitative physical arguments presented in [20].

In Fig. 1 only the case of purely diffuse accommodation is presented. The DSMC decomposition may also be applied in the case of Maxwell boundary conditions. In this latter case the indicator of the particles following a specular reflection at the wall is not set equal to 0 (as is done with the diffuse reflection) and on the contrary remains the same as before the specular reflection. Beyond that the methodology is identical and the values of $\delta$ where the Knudsen minimum occurs for $\alpha < 1$ are accordingly obtained and justified.

The behavior of the ballistic and collision velocity distributions is according to the corresponding flow rate results; i.e., as $\delta$ is increased, $u^{(b)}$ is decreased, while $u^{(c)}$ is increased. At $\delta = 0.1$, $u^{(b)}(x)$ is larger than $u^{(c)}(x)$, then at $\delta = 1$ is smaller but remains large enough compared to $u^{(c)}$, while at $\delta = 5$ becomes negligibly small.

More interesting is the partition of the number density into its ballistic and collision segments which are plotted, scaled to the average sampled initial density, in Fig. 3 for channel flow with $\delta = [0.1,1,5]$. All distributions are symmetric about $x = 0.5$ and thus only half of the flow domain is shown. The overall number density $n(x) = n^{(b)} + n^{(c)} = 1$ is always constant. For all $\delta$, $n^{(b)}(x)$ has its largest values at the walls ($x = 0,1$) and it decreases moving towards the center of the channel, taking its lowest values at $x = 0.5$, while $n^{(c)}(x) = 1 - n^{(b)}$ behaves in an exactly opposite manner. For the ballistic particle distribution the boundaries act as a source, while the bulk flow acts as a sink and the situation is reversed for the collision

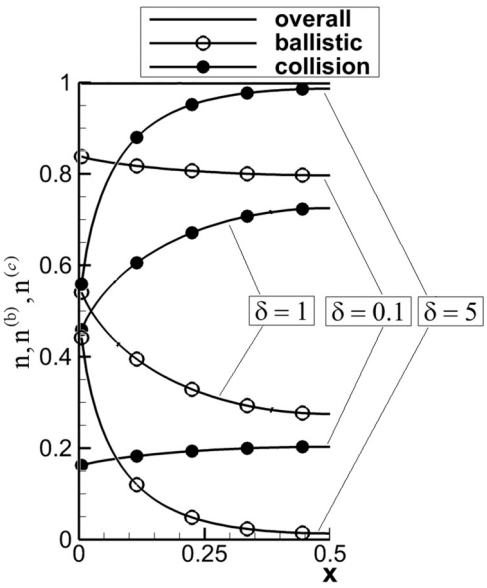


FIG. 3. Number density distributions for channel flow and various values of $\delta$.

TABLE II. Dimensionless average wall shear stress for the channel and tube flows.

| | Channel | | | Tube | | |
|---|---|---|---|---|---|---|
| $\delta$ | $\bar{\tau}_{xz}$ | $\bar{\tau}_{xz}^{(b)}$ | $\bar{\tau}_{xz}^{(c)}$ | $\bar{\tau}_{rz}$ | $\bar{\tau}_{rz}^{(b)}$ | $\bar{\tau}_{rz}^{(c)}$ |
| 0.01 | 2.47(–1) | 2.40(–1) | 7.00(–3) | 2.49(–1) | 2.45(–1) | 4.83(–3) |
| 0.1 | 2.48(–1) | 2.13(–1) | 3.48(–2) | 2.49(–1) | 2.13(–1) | 3.71(–2) |
| 1 | 2.47(–1) | 1.45(–1) | 1.03(–1) | 2.49(–1) | 1.25(–1) | 1.25(–1) |
| 5 | 2.47(–1) | 1.13(–1) | 1.34(–1) | 2.48(–1) | 1.06(–1) | 1.42(–1) |
| 10 | 2.46(–1) | 1.08(–1) | 1.39(–1) | 2.48(–1) | 1.03(–1) | 1.42(–1) |

particle distribution, where the bulk flow acts as a distributed source and the walls as a sink. The overall behavior of the ballistic and collision number densities in terms of $\delta$ is similar to the one of the velocities. Note that even at $\delta = 5$, although at the center of the channel $n^{(b)}$ is negligible small compared to $n^{(c)}$, close to the boundaries is lower but still close to $n^{(c)}$. The region next to the boundaries where $n^{(b)}$ is nonzero corresponds to the Knudsen layer.

Tabulated results of the dimensionless average wall shear stresses are given in Table II for the channel and tube flows. The overall stresses $\bar{\tau}_{\alpha z}$ are independent of $\delta$ and they are slightly lower than the analytical result of 0.25, since they are calculated, as all macroscopic quantities, at the center of each cell. As $\delta$ is increased $\bar{\tau}_{\alpha z}^{(b)}$ decreases and $\bar{\tau}_{\alpha z}^{(c)}$ increases, with $\bar{\tau}_{\alpha z}^{(b)}$ remaining important as a wall quantity even at $\delta = 5$, while its contribution to $\bar{\tau}_{\alpha z}$ far from the wall at the same $\delta$ rapidly vanishes.

The well-known Knudsen paradox has been investigated by decomposing the particle distribution function into its ballistic and collision parts and examining the effect of each part to the overall solution. It has been shown in a precise quantitative manner that the difference in the rate of change of the corresponding ballistic and collision flow rates with respect to the rarefaction parameter yields the Knudsen minimum of the overall reduced flow rate or conductance.

[1] M. Knudsen, Die Gesetze der Molekularströmung und der inneren Reibungsströmung der Gase durch Röhren, Ann. Phys. **333**, 75 (1909).

[2] T. Ohwada, Y. Sone, and K. Aoki, Numerical analysis of the Poisseuille and thermal transpiration flows between two parallel plates on the basis of the Boltzmann equation for hard-sphere molecules, Phys. Fluids A **1**, 2042 (1989).

[3] K. Aoki, Numerical analysis of rarefied gas flows by finite-difference method, in *Rarefied Gas Dynamics*, Vol. 118, edited by E. P. Muntz, D. P. Weaver, and D. H. Campbell (AIAA, Washington, DC, 1989), p. 297.

[4] S. A. Tison, Experimental data and theoretical modeling of gas flows through metal capillary leaks, Vacuum **44**, 1171 (1993).

[5] S. K. Loyalka and S. A. Hamoodi, Poiseuille flow of a rarefied gas in a cylindrical tube: Solution of linearized Boltzmann equation, Phys. Fluids **2**, 2061 (1990).

[6] F. M. Sharipov and V. D. Seleznev, Rarefied gas flow through a long tube at any pressure ratio, J. Vac. Sci. Technol. A **12**, 2933 (1994).

[7] D. Valougeorgis, The friction factor of a rarefied gas flow in a circular tube, Phys. Fluids **19**, 091701 (2007).

[8] S. Varoutis, S. Naris, V. Hauer, C. Day, and D. Valougeorgis, Experimental and computational investigation of gas flows through long channels of various cross sections in the whole range of the Knudsen number, J. Vac. Sci. Technol. A **27**, 89 (2009).

[9] J. Pitakarnnop, S. Varoutis, D. Valougeorgis, S. Geoffroy, L. Baldas, and S. Colin, A novel experimental setup for gas microflows, Microfluid. Nanofluid. **8**, 57 (2010).

[10] P. Perrier, I. A. Graur, T. Ewart, and J. G. Meolans, Mass flow rate measurements in microtubes: From hydrodynamic to near free molecular regime, Phys. Fluids **23**, 042004 (2011).

[11] A. Ganguly, S. L. Nail, and A. A. Alexeenko, Experimental determination of the key heat transfer mechanisms in pharmaceutical freeze drying, J. Pharm. Sci. **102**, 1610 (2013).

[12] S. Naris, C. Tantos, and D. Valougeorgis, Kinetic modeling of a tapered Holweck pump, Vacuum **109**, 341 (2014).

[13] S. Pantazis and K. Jousten, Computational and experimental study of unsteady gas flow in a dynamic vacuum standard, Vacuum **109**, 373 (2014).

[14] A. Ketsdever, N. Gimelshein, S. Gimelshein, and N. Selden, Radiometric phenomena: From the 19th to the 21st century, Vacuum **86**, 1644 (2012).

[15] H. Struchtrup and M. Torrilhon, Higher-order effects in rarefied channel flows, Phys. Rev. E **78**, 046301 (2008).

[16] W. P. Yudistiawan, S. K. Kwak, D. V. Patil, and S. Ansumali, Higher-order Galilean-invariant lattice Boltzmann model for microflows: Single-component gas, Phys. Rev. E **82**, 046701 (2010).

[17] S. Kokou Dadzie and H. Brenner, Predicting enhanced mass flow rates in gas microchannels using nonkinetic models, Phys. Rev. E **86**, 036318 (2012).

[18] M. A. Gallis and J. R. Torczynski, Direct simulation Monte Carlo-based expressions for the gas mass flow rate and pressure profile in a microscale tube, Phys. Fluids **24**, 012005 (2012).

[19] F. Sharipov and I. Graur, General approach to transient flows of rarefied gases through long capillaries, Vacuum **100**, 22 (2014).

[20] W. G. Pollard and R. D. Present, On gaseous self-diffusion in long capillary tubes, Phys. Rev. **73**, 762 (1948).

[21] M. Vargas, G. Tatsios, D. Valougeorgis, and S. Stefanov, Rarefied gas flow in a rectangular enclosure induced by non-isothermal walls, Phys. Fluids **26**, 057101 (2014).

[22] G. Tatsios, M. Vargas, D. Valougeorgis, and S. Stefanov, Non-equilibrium gas flow and heat transfer in a heated square microcavity, Heat Transfer Eng. (to be published).

[23] K. Aoki, P. Degond, S. Takata, and H. Yoshida, Diffusion models for Knudsen compressors, Phys. Fluids **19**, 117103 (2007).

[24] F. Sharipov and V. Seleznev, Data on internal rarefied gas flows, J. Phys. Chem. Ref. Data **27**, 657 (1998).

[25] F. Sharipov, Rarefied gas flow through a long rectangular channel, J. Vac. Sci. Technol. A **17**, 3062 (1999).

[26] I. Graur and F. Sharipov, Gas flow through an elliptical tube over the whole range of the ga rarefaction, Eur. J. Mech. B/Fluids **27**, 335 (2008).

[27] G. Breyiannis, S. Varoutis, and D. Valougeorgis, Rarefied gas flow in concentric annular tube: Estimation of the Poiseuille number and the exact hydraulic diameter, Eur. J. Mech. B/Fluids **27**, 609 (2008).

[28] G. A. Bird, *Molecular Gas Dynamics and the Direct Simulation of Gas Flows* (Clarendon, Oxford, 1994).